Research Article

Received: 1 September 2011 Revised: 1 November 2011 Accepted: 1 November 2011 Published online in Wiley Online Library: 30 January 2012

(wileyonlinelibrary.com) DOI 10.1002/pi.4149

Improvements of electromechanical properties of gelatin hydrogels by blending with nanowire polypyrrole: effects of electric field and temperature

Thawatchai Tungkavet,[a] Nispa Seetapan,[b] Datchanee Pattavarakorn[c] and Anuvat Sirivat[a]*

Abstract

Nanowire-polypyrrole/gelatin hydrogels were fabricated by dispersion of nanowire-polypyrrole into a gelatin aqueous solution followed by solvent casting. The electromechanical properties, thermal properties and deflection of pure gelatin hydrogel and nanowire-polypyrrole/gelatin hydrogels were studied as functions of temperature, frequency and electric field strength. The 0.01%, 0.1%, 0.5%, 1% v/v nanowire-polypyrrole/gelatin hydrogels and pure gelatin hydrogel possess storage modulus sensitivity values of 0.75, 1.04, 0.88, 0.99 and 0.46, respectively, at an electric field strength of 800 V mm^{-1}. The effect of temperature on the electromechanical properties of the pure gelatin hydrogel and nanowire-polypyrrole/gelatin hydrogels was investigated between 30 and 80 °C; there are three regimes for the storage modulus behaviour. In deflection testing in a cantilever fixture, the dielectrophoresis force was determined and found to increase monotonically with electric field strength. The pure gelatin hydrogel shows the highest deflection angle and dielectrophoresis force at an electric field strength of 800 V mm^{-1} relative to those of the nanowire-polypyrrole/gelatin hydrogels.

Keywords: biopolymer; gelatin; hydrogels; conducting polymers; actuator

INTRODUCTION

The exchange of electrical energy and mechanical energy has been of scientific and technological interest for many decades. Electroactive polymers offer promising and novel characteristics such as light weight, high energy density and high flexibility. They are also candidates for muscle-like actuator materials. Some of the currently available materials are ionic polymer–metal composites,[1] gel polymers,[2] conductive polymers,[3] electric field activated electroactive polymers such as electron irradiated polyvinylidene fluoride trifluoroethylene polymers,[4] dielectric elastomers,[5] electrostrictive polymer artificial muscle[6,7] and electro-rheological fluids.[8] The development of electroactive materials for artificial muscles or actuators is sought after because of the benefits they offer.

Gelatin is one type of electroactive polymer; it is a protein biopolymer derived from the partial hydrolysis of native collagens, the most abundant structural proteins found in the animal body: skin, tendons, cartilage and bone. It is a good film- and particle-forming material.[9] Due to its many merits – its biological origin, non-immunogenicity, biodegradability, biocompatibility and commercial availability at relatively low cost – gelatin has been widely used in the pharmaceutical and medical fields as sealants for vascular prostheses, carriers for drug delivery, wound dressings and artificial muscles.[10] Normally gelatin is produced by denaturing a naturally derived collagen in solution through either an acidic or alkaline process in which the triple-helix structure is separated into a random coil structure. During the gelling process, the random coil in a warm aqueous solution will change into a coil–helix structure when cooled.[11] However, gelatin exhibits poor mechanical properties, which limits its possible application as a biomaterial. In order to use this material in practical applications, the structure needs to be reinforced either through crosslinking or by using some filler materials. However, the presence of residual crosslinking agents can lead to toxic side effects. The use of multiwall carbon nanotubes as a reinforcement in gelatin has been studied by Haider *et al*.[12] Recently, the insertion of a conductive polymer into a biopolymer forming a blend has been of keen interest. Conductive polymers can offer a variety of benefits to the host biopolymer: variable conductivity and better thermal stability and mechanical properties.[13] On the other hand, conducting polymers have been intensively studied for their one-dimensional conjugated structures and adjustable conductivity.[14]

* *Correspondence to: Anuvat Sirivat, Conductive and Electroactive Polymers Research Unit, Petroleum and Petrochemical College, Chulalongkorn University, Soi Chula 12, Phyathai Rd, Bangkok 10330, Thailand. E-mail: anuvat.s@chula.ac.th; www.cepru.research.ac.th*

a *Petroleum and Petrochemical College, Chulalongkorn University, Bangkok 10330, Thailand*

b *National Metal and Materials Technology Center, Pathumthani 12120, Thailand*

c *Department of Industrial Chemistry, Faculty of Science, Chiang Mai University, Chiangmai 50200, Thailand*

Among the conducting polymers, polypyrrole (Ppy) is one of the most investigated due to its high electrical conductivity, relatively good environmental stability and low toxicity.[15–17] Also, the synthesis of nanoscale materials has attracted great interest during the past 10 years. Chemical oxidation polymerization is simple and cheap in producing large quantities of nanostructural Ppy, because it overcomes the limitation of electrochemical polymerization. Duchet *et al*.[18] used commercial polycarbonate nanoporous particle track-etched membranes as templates to prepare Ppy nanotubules and nanofibrils.

In the present study, we were interested in blending nanowire-polypyrrole (nanowire-Ppy) as a conductive polymer with a gelatin hydrogel containing an ionic surfactant (i.e. dodecylbenzene sulfonic acid (DBSA) dispersed in an aqueous solvent). The mechanical properties, electromechanical properties and electrical properties were investigated in terms of nanowire-Ppy concentration, electric field strength and temperature.

MATERIALS AND METHODS

Materials

Gelatin (type B, bovine skin), pyrrole monomer (Sigma) and calcium hydride (Fluka) were used as received. Anhydrous iron(III) chloride (Riedel-de Hean) was used as an oxidant without further purification. DBSA (Sigma) was used as received as a dopant.

Synthesis of nanowire-polypyrrole

In this work, we followed the chemical synthesis procedure of He *et al*.[19] for the nanowire-Ppy. The pyrrole monomer was dried by mixing with CaH_2 in a ratio of 100 g of CaH_2 per litre of pyrrole and the reaction was allowed to proceed for 24 h. Then 0.0175 mol DBSA and 0.0175 mol of dried pyrrole monomer were dissolved in separate beakers of 250 mL of distilled water. The solutions were mixed together by vigorously stirring to obtain an emulsion. A solution of $FeCl_3$ (0.065 mol, 0.01625 mol L^{-1}) in deionized water was added to the emulsion at 0 °C for a duration of 40 h. It was terminated by pouring a large excess of methanol into the solution. The resulting Ppy precipitate was vacuum filtered and washed with methanol, acetone and distilled water several times until the pH was equal to 6.0. Finally, it was dried in a vacuum oven for 40 h at 30 °C. Other Ppys were synthesized with the same procedure but with 0.000175, 0.00175, 0.175, 0.875 and 1.75 mol DBSA.

Preparation of the nanowire-polypyrrole/gelatin hydrogel

The various concentrations of nanowire-Ppy (0.01%, 0.1%, 0.5% and 1% v/v) were dispersed by a transonicator (Elma, D 7284) in an aqueous medium filled with 4×10^{-3} mol L^{-1} DBSA. Then the gelatin hydrogel was prepared by dissolution in 10% v/v distilled water (pH 6.40) at 40 °C overnight by magnetic stirring until the pH was equal to 6.31. The two solutions were mixed and poured onto a Petri dish for the hydrogel casting at room temperature. The thickness of the hydrogel samples was about 1.4 mm. Figure 1 shows a schematic diagram for the possible interaction of the gelatin and DBSA.

Characterization and testing of composite hydrogels

Each Ppy sample was identified for functional groups by Fourier transform infrared spectroscopy (FTIR) (Thermo Nicolet, Nexus 670) operated in the absorption mode with 32 scans and a resolution of ± 4 cm^{-1}, covering a wavenumber range from 3500 to 500 cm^{-1} using a deuterated triglycine sulfate detector. Optical grade potassium bromide (Carlo Erba reagent) was used as the background material.

Electrical conductivity was measured with a meter which consisted of two probes that made contact with the surface of the film sample. The probes were connected to a source meter (Keithley, Model 6517A) for a constant voltage source and for reading the current. The applied voltage and the resultant current in the linear ohmic regime were used to determine the electrical conductivity of the polymer using the equation

$$\sigma = \frac{1}{\rho} = \frac{1}{R_s t} = \frac{1}{KVI} \quad (1)$$

where σ is the specific conductivity (S cm^{-1}), ρ is the specific resistivity (Ω cm), R_s is the sheet resistivity (Ω), I is the measured current (A), K is the geometric correction factor, V is the applied voltage (V) and t is the pellet thickness (cm).

Scanning electron micrographs were taken with a scanning electron microscope (JEOL, model JSM-5200) to determine the morphology of the Ppy in powder form at various DBSA concentrations. The micrographs of Ppy were obtained by using an acceleration voltage of 15 kV with magnifications of 15 000 and 100 000 times.

AFM (CSPM 4000) images were taken with a scanning electron microscope to determine the topology of the hydrogels at various concentrations of nanowire-Ppy by using a scan rate 0.5 Hz and a scan size of 10 μm × 10 μm.

A melt rheometer (Rheometric Scientific, ARES) was used to measure the rheological properties. It was fitted with a custom-built copper parallel plate fixture (diameter 30 mm). A DC voltage was applied with a DC power supply (Instek, GFG8216A), which can deliver an electric field strength to 800 V mm^{-1}. A digital multimeter was used to monitor the voltage input. In these

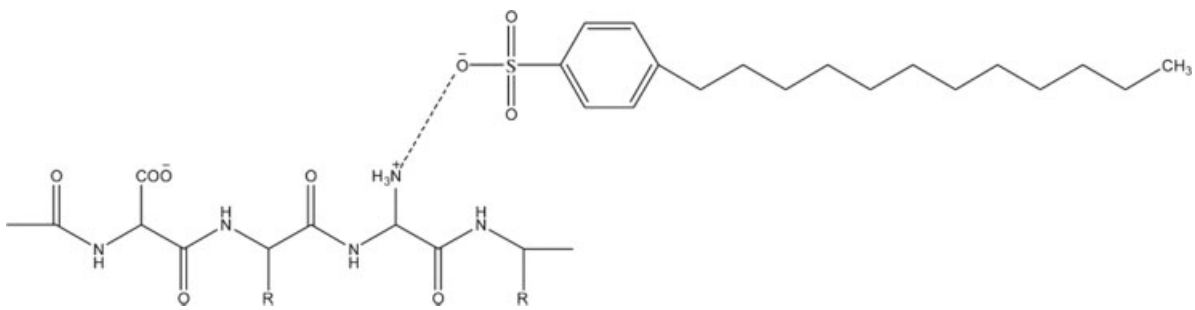

Figure 1. Scheme of the possible interaction of the gelatin and DBSA.

experiments, the oscillatory shear strain was applied and the dynamic moduli (G' and G'') were measured as functions of frequency and electric field strength. Strain sweep tests were first carried out to determine suitable strains to measure G' and G'' in the linear viscoelastic regime. The appropriate strain was determined to be 0.15% for both the pure gelatin hydrogels and the nanowire-Ppy/gelatin hydrogels. Then frequency sweep tests were carried out to measure G' and G'' for each sample as functions of frequency. The deformation frequency was varied from 0.1 to 100 rad s^{-1}. Before each measurement, pure gelatin hydrogels and nanowire-Ppy/gelatin hydrogels were pre-sheared at a low frequency (0.039811 rad s^{-1}), and then the electric field was applied for 15 min to ensure the formation of equilibrium polarization before taking the G' and G'' measurements. Experiments were carried out at a temperature of 30 °C and repeated at least two to three times. The effect of temperature was studied at various temperatures between 30 and 80 °C for the pure gelatin hydrogels and the nanowire-Ppy/gelatin hydrogels. The temporal response experiments were carried out at 800 V mm^{-1}. Deflections of the pure gelatin hydrogel and the nanowire-Ppy/gelatin hydrogels were carried out under various applied electric field strengths. For each hydrogel, one end of the sample was fixed with a grip vertically in a transparent chamber containing two parallel electrodes. The input DC field was provided by a DC power supply (Gold Sun 3000, GPS 3003D) and a high voltage power supply (Gamma High Voltage, UC5-30P), which delivered various electric field strengths from 25 to 600 V mm^{-1}. A digital video recorder (Sony, Handicam HR1) was used to record the displacement of the films. The tip displacement was measured and calculated from a Scion Image (Beta 4.0.3) program.

From the static force balance, the deflecting force or the dielectrophoresis force (F_d) on the samples is equal to the sum of the resisting elastic force (F_e) and the weight along the bending direction (Eqn (2)), where the film deflection distance at equilibrium is d.

$$F_d = F_e + mg\sin\theta \tag{2}$$

where m is the sample's mass (kg), g is the gravity constant (9.8 m s^{-2}), θ is the deflection angle and F_e is the resisting elastic force (N). In our experiment, the film deflections were small. The linear deflection theory of one free-end film was therefore used where the elastic force can be calculated using the equation[20,21]

$$F_e = \frac{dEI}{l^3} \tag{3}$$

where E is the elastic modulus which is equal to $2G'(1+\nu)$ in which G' (1 rad s^{-1}, E) is the shear modulus and ν is Poisson's ratio, equal to 1/2 for an incompressible material, I is the moment of inertia, equal to $t^3w/12$, where t is the sample thickness and w is the sample width, d is the deflection distance and l is the sample length.

RESULTS AND DISCUSSION

Characterization of nanowire-polypyrrole

An FTIR spectrum of the Ppy was taken to identify the characteristic absorption peaks, as shown in Table 1; the characteristic peaks of the synthesized Ppy are at 1547, 1450, 1302, 1178, 1038 and 633 cm^{-1}. The pyrrole ring vibration occurs at 1547 and 1450 cm^{-1},[19] the =C–H in-plane vibration at 1302 and 1038 cm^{-1},[19] and the C–N stretching vibration at 1178 cm^{-1}.[22]

Table 1. FTIR characteristic peaks of synthesized Ppy

Wavenumber (cm^{-1})	Assignment
1547, 1450	Pyrrole ring
1302, 1038	=C–H in plane
1178	C–N stretching
633	Sulfonate anion

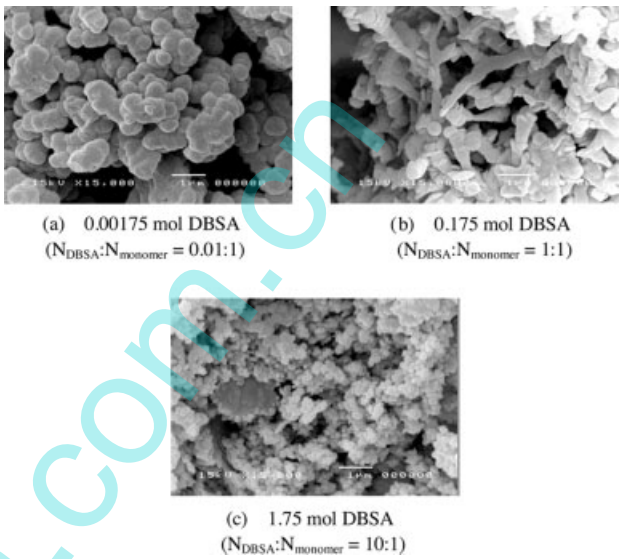

Figure 2. SEM micrographs of DBSA-doped synthesized Ppy at various DBSA concentrations with a magnification of 15000 (a) 0.0175 mol (N_{DBSA} : $N_{monomer}$ = 0.01 : 1); (b) 0.175 mol (N_{DBSA} : $N_{monomer}$ = 1 : 1); (c) 1.750 mol (N_{DBSA} : $N_{monomer}$ = 10 : 1).

When Ppy is doped with DBSA, the peak at 633 cm^{-1} increases. This peak represents the S=O and S–O stretching vibrations of sulfonate anions which compensate for the positive charges in the Ppy chains.[23]

The effect of the doping level on the morphology of the conductive polymer was investigated by SEM. Figure 2 shows micrographs of synthesized Ppy with various DBSA concentrations: 0.00175 to 1.75 mol (N_{DBSA} : $N_{monomer}$ to 0.01 : 1, 1 : 1, and 10 : 1). It is interesting to observe that upon increasing the dopant level the morphology of the conductive polymer changes from having a typical three-dimensional random coil nanogranular structure to a nanowire fibrillar structure and then returns to a nanogranular structure again (Figs 2(a)–2(c)). The micrographs suggest that as the dopant concentration increases more polarons and bipolarons are generated along the polymer chains and they induce a granule-to-nanowire transition. It can be seen that the concentration of DBSA strongly affects the morphology of the Ppy obtained. When the concentration of DBSA in the reaction solution is higher than 0.175 mol, the resulting morphology of Ppy is granular, similar to that of Ppy synthesized with other dopants.[23–25] As previously mentioned, the nanowire-Ppy is obtained when the reacting solution is at a proper reactant concentration, and nanogranular Ppy is obtained with a higher reactant concentration.[26] The resulting Ppy average particle sizes for various DBSA concentrations (N_{DBSA} : $N_{monomer}$ equal to 0.01 : 1, 0.1 : 1, 0.5 : 1, 1 : 1, 5 : 1 and 10 : 1) are tabulated in Table 2. Figure 3 shows micrographs of the cross-sections of the

Table 2. Average particle sizes and electrical conductivity data of Ppy synthesized with different DBSA/pyrrole ratios

Concentration of DBSA and pyrrole ratio (N_{DBSA} : $N_{monomer}$)	Average particle size (nm)	Conductivity (S cm^{-1})
0.01 : 1	370 ± 28.10	0.76 ± 0.0002
0.1 : 1	250 ± 40.30	1.37 ± 0.0009
0.5 : 1	195 ± 14.20	2.30 ± 0.0023
1 : 1	95 ± 18.00	23.86 ± 0.032
5 : 1	53 ± 4.10	15.41 ± 0.018
10 : 1	49 ± 2.60	15.95 ± 0.011

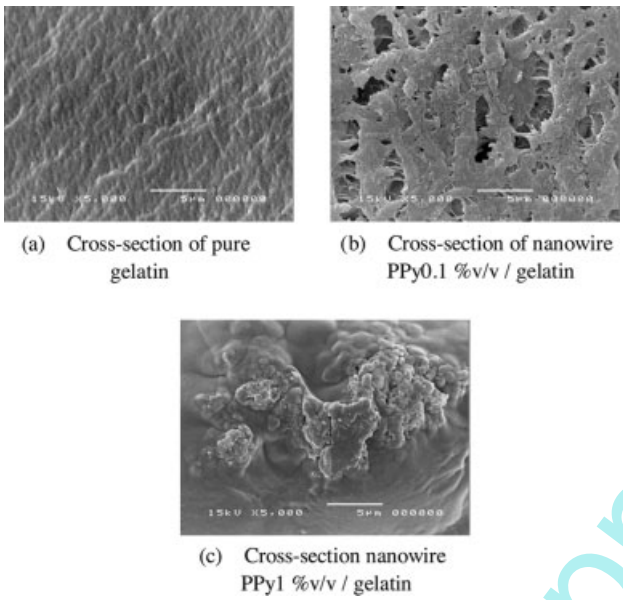

Figure 3. SEM micrographs of cross-sections of the pure gelatin and the nanowire-Ppy/gelatin hydrogels: (a) cross-section of the pure gelatin; (b) cross-section of the 0.1 vol% nanowire-Ppy/gelatin; and (c) cross-section of the 1 vol% nanowire-Ppy/gelatin.

nanowire-Ppy/gelatin hydrogels at various nanowire-Ppy concentrations. The nanowire-Ppy shows a moderate dispersion in the gelatin solution at low nanowire-Ppy concentrations with the aid of the surfactant; the dispersion becomes relatively poor at high nanowire-Ppy concentrations. Partially homogeneous nanowire-Ppy/gelatin hydrogel is obtained due to the poor nanowire-Ppy dispersion as a result of the van der Waals forces between Ppy nanowires.

The specific electrical conductivity of Ppy and nanowire-Ppy was measured with a custom-built two-point probe (Keithley, Model 6517A). The specific electrical conductivity with corresponding standard deviations of Ppy, at N_{DBSA} : $N_{monomer}$ equal to 0.01 : 1, 0.1 : 1, 0.5 : 1, 1 : 1, 5 : 1 and 10 : 1, is shown in Table 2. The electrical conductivity of Ppy is thus closely related to its morphology. The conductivity (σ) is expressed as $\sigma = ne\mu$ where n is the density of charge carriers, e represents the electron charge and μ is the mobility of the charge carriers. Thus, the electrical conductivity of Ppy is proportional to the density (the doping level in the case of conducting polymers) and the mobility of the charge carriers. The conductivity of nanogranular Ppy (10 : 1) is 15.95 S cm^{-1}, lower than that of nanowire-Ppy (1 : 1) which is 23.86 S cm^{-1}. Ppy with nanowire morphology presumably has a higher mobility for the charge carriers than granular Ppy and this factor dominates the charge carrier density factor.[27]

The topology and the orientation of the nanowire-Ppy/gelatin hydrogels were also investigated by AFM. The AFM micrographs of the nanowire-Ppy/gelatin and the pure gelatin hydrogels are demonstrated in Figs 4(a)–4(c). Figure 4(a) shows the topology and the orientation of the 0.1% v/v nanowire-Ppy/gelatin hydrogel; it consists of nanorods which are aligned in one direction with a uniform distribution by a mechanical force; the schematic diagram is illustrated in Fig. 4(a′). The 1% nanowire-Ppy/gelatin hydrogel possesses a cottage-like topology is aggregation of conductive polymer. Its topology presumably consists of nanowires piling up randomly on each other as shown in Fig. 4(b) and in the schematic diagram in Fig. 4(b′) due to the agglomeration. The topology of the pure gelatin hydrogel is shown in Fig. 4(c). Figure 4(a) of the 0.1% v/v nanowire-Ppy/gelatin hydrogel shows that the nanowire-Ppy is dispersed quite uniformly within the gelatin hydrogel.

Electromechanical properties

Time dependence of the electro-rheological response

We investigated the temporal characteristics of the pure gelatin and the nanowire-Ppy/gelatin hydrogels (0.1% and 1% v/v) at an electric field strength of 800 V mm^{-1} from the time sweep tests, in which the electric field was turned on and off alternately. The temporal characteristic of each sample was recorded in the linear viscoelastic regime at a strain of 0.15% and a frequency of 100 rad s^{-1}. Figure 5 shows a comparison of the storage modulus G' of the pure gelatin and of the nanowire-Ppy/gelatin hydrogels during the time sweep tests. At an electric field strength of 800 V mm^{-1}, G' immediately increases and rapidly reaches a steady-state value. For the pure gelatin hydrogel, when the electric field is turned off, G' decreases instantaneously to its original state. For the nanowire-Ppy/gelatin hydrogel (0.1% and 1% v/v), G' decreases but does not recover its original value. This behaviour indicates that there are some irreversible agglomerations of the nanowire-Ppy or some dipole moment residues, possibly due to some hydrogen bonding between adjacent nanowire-Ppy. However, the 1% v/v nanowire-Ppy/gelatin hydrogel shows a quick response under an electric field since the agglomeration of nanowire-Ppy in hydrogels constitutes large induced dipole moment domains.

Effect of electric field strength and concentration

The effect of electric field strength on the electromechanical properties of the nanowire-Ppy/gelatin hydrogels of 0, 0.01, 0.1, 0.5 and 1 vol% were investigated in the range 0–800 V mm^{-1}. Figure 6 shows the storage modulus response ($\Delta G'$) of the hydrogels *versus* electric field strength at a frequency of 100 rad s^{-1}, a strain of 0.15% and a temperature of 30 °C. The increases in $\Delta G'$ with electric field strength are nonlinear within the range 0.1–800 V mm^{-1}. The storage modulus response values of these samples at an electric field strength of 800 V mm^{-1} are 250 000, 503 000, 1 005 000, 212 990 and 202 779 Pa for the pure gelatin, the nanowire-Ppy(0.01 vol%)/gelatin, the nanowire-Ppy(0.1 vol%)/gelatin, the nanowire-Ppy(0.5 vol%)/gelatin and the nanowire-Ppy(1 vol%)/gelatin hydrogels, respectively. (The storage modulus sensitivity values of these samples at an electric field strength of 800 V mm^{-1} are tabulated in Table 3.) The mixing of the nanowire-Ppy into gelatin leads to increases in G' with and without an electric field. The increase of G'_o can be attributed to the effect of particles acting as fillers. For the small amount

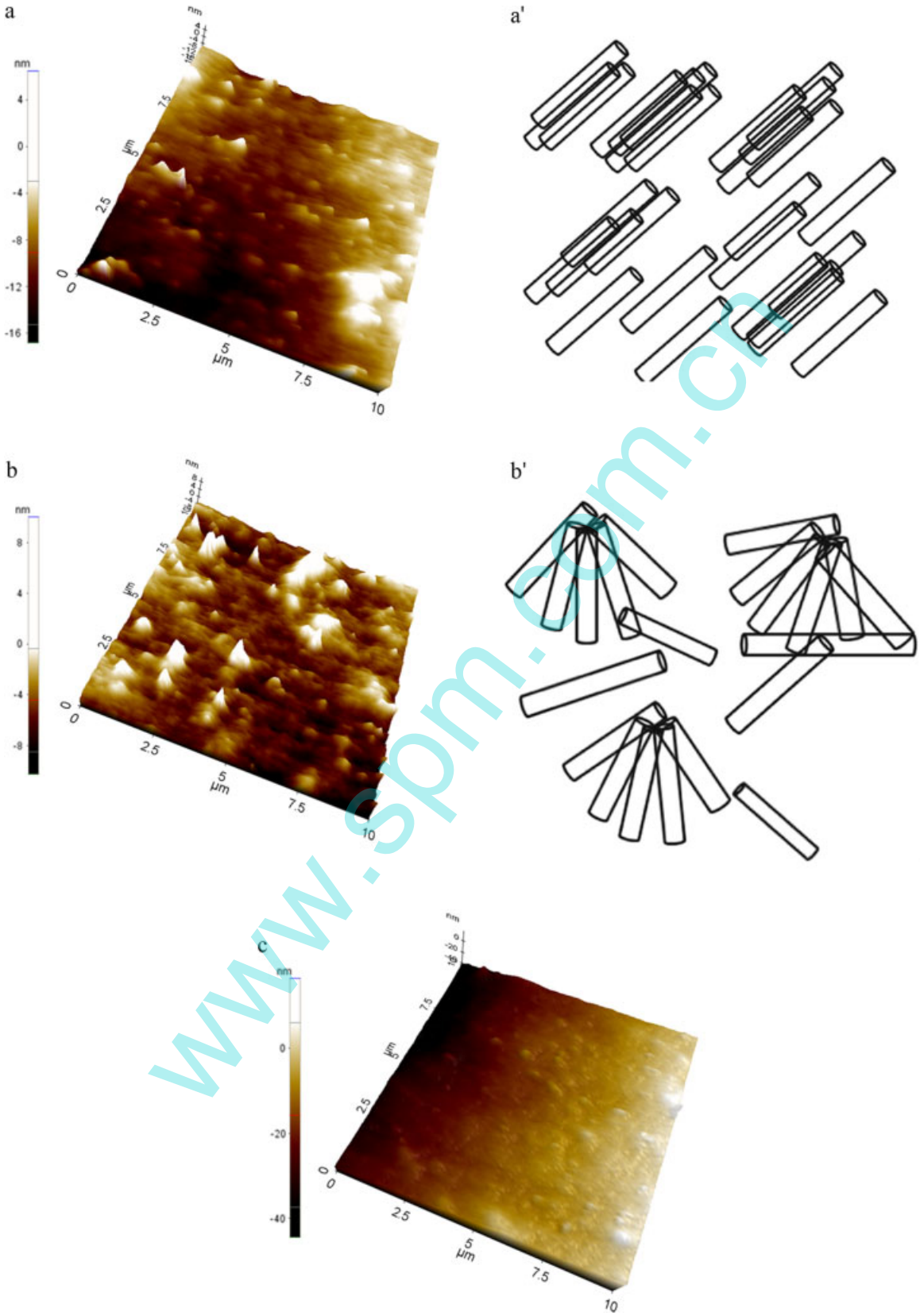

Figure 4. (a) AFM micrograph of nanowire-Ppy(0.1 vol%)/gelatin hydrogel; (a′) schematic diagram of the orientation of nanowire-Ppy(0.1 vol%); (b) AFM micrograph of nanowire-Ppy(1 vol%)/gelatin hydrogel; (b′) schematic diagram of the orientation of nanowire-Ppy(1 vol%); (c) AFM micrograph of pure gelatin hydrogel.

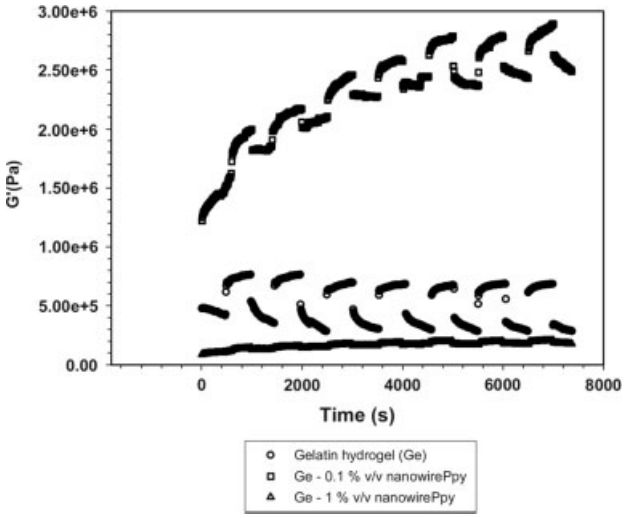

Figure 5. Temporal responses of the storage modulus (G') of the pure gelatin hydrogel and the nanowire-Ppy/gelatin hydrogels (sample diameter 30 mm, gel thickness 1.405 mm, 0.15% strain, frequency 100 rad s^{-1}, electric field strength 800 V mm^{-1}, 30 °C): ○, pure gelatin hydrogel; □, 0.1 vol% nanowire-Ppy; △, 1 vol% nanowire-Ppy.

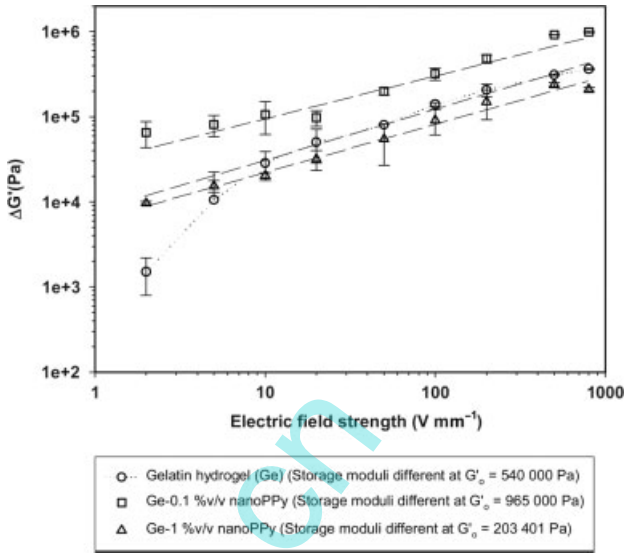

Figure 6. Effect of concentration of particles on the storage modulus response ($\Delta G'$) at various electric field strengths (sample diameter 30 mm, gel thickness 1.405 mm, 0.15% strain, frequency of 100 rad s^{-1}, 30 °C): ○, pure gelatin hydrogel; □, 0.1 vol% nanowire-Ppy; △, 1 vol% nanowire-Ppy.

of nanowire-Ppy added, the fillers induce only an additional free volume, but the distances between particles are large enough to create a significant particle interaction through the electric-field-induced dipole moments.[28] Therefore, the storage modulus sensitivity becomes high only at suitable nanowire-Ppy concentrations. The maximum $\Delta G'$ and $\Delta G'/G'_o$ occurs with the nanowire-Ppy(0.1 vol%)/gelatin hydrogel. However, the storage modulus response and sensitivity decrease with a nanowire-Ppy concentration greater than 0.1 vol%. For the hydrogel system with the highest particle concentration of 1 vol%, the storage modulus response under the effect of the electric field diminishes since the hydrogel presumably involves phase separation between the gelatin hydrogel and the nanowire-Ppy agglomeration.

Liu and Shaw[29] reported a similar effect for a silica/silicone system. The enhancement of the shear modulus was negligible below 8.0 vol% but increased dramatically above this threshold concentration. Above 55 vol%, the shear modulus decreased since the interparticle force decreased with the steric hindrance effect. Kunanuruksapong and Sirivat[30] found that the storage modulus of a polymer blend between poly(*p*-phenylene) and an acrylic elastomer increased with increasing poly(*p*-phenylene) concentration. However, at the higher particle concentration of 30 vol%, the storage modulus response ($\Delta G'_{2kV/mm}$) decreased.

Effect of the operating temperature

The mechanical properties of the pure gelatin and the nanowire-Ppy/gelatin hydrogels in an electric field were investigated at operating temperatures between 30 and 80 °C. G' and $\Delta G'$ (100 rad s^{-1}) are plotted against temperature in Fig. 7. One sample was used for each of the G'_o and G' measurements. An electric field was first applied on another sample for a period of 10 min before G' was measured successively at each temperature. Experiments were carried out using two representative hydrogels, pure gelatin and nanowire-Ppy(0.1 vol%)/gelatin hydrogel, as shown in Fig. 7. Figure 7 shows that the storage modulus of the pure gelatin hydrogel initially decreases in the temperature range 30–40 °C because of the denaturation of the triple-helix coil to a random coil.[31] In the temperature range 40–60 °C, the storage modulus increases, consistent with classical network theory.[20] The higher temperature induces more entropy of the gel, leading to an increase in the retractive force and the storage modulus. However, the storage modulus decreases with increasing temperature between 60 and 80 °C, the temperature range close to the low temperature glasss transition of 120 °C in which the devitrification of α-amino acid block occurs.[32] In the case of 0.1% nanowire-Ppy/gelatin hydrogel, the temperature increment under an electric field retards the denaturation temperature (30–40 °C) and the low temperature glass transition (60–80 °C) because of the polarization of Ppy. In addition, the storage modulus

Table 3. Sensitivity of the storage modulus of the pure gelatin and the nanowire-Ppy/gelatin hydrogels: 0.15% strain, electric field strength 800 V mm^{-1}, frequency 100 rad s^{-1}, at 30 °C

Material (nanowire-Ppy diameter 95 ± 18 nm)	Storage modulus (G') (Pa)	Initial storage modulus (G'_o) (Pa)	Sensitivity of storage modulus ($\Delta G'/G'_o$) (Pa)
Gelatin hydrogel (Ge)	790 000	540 000	0.46
Ge–0.01 vol% nanowire-Ppy	1 170 000	667 000	0.75
Ge–0.1 vol% nanowire-Ppy	1 970 000	965 000	1.04
Ge–0.5 vol% nanowire-Ppy	447 100	234 010	0.88
Ge–1 vol% nanowire-Ppy	406 180	203 401	0.99

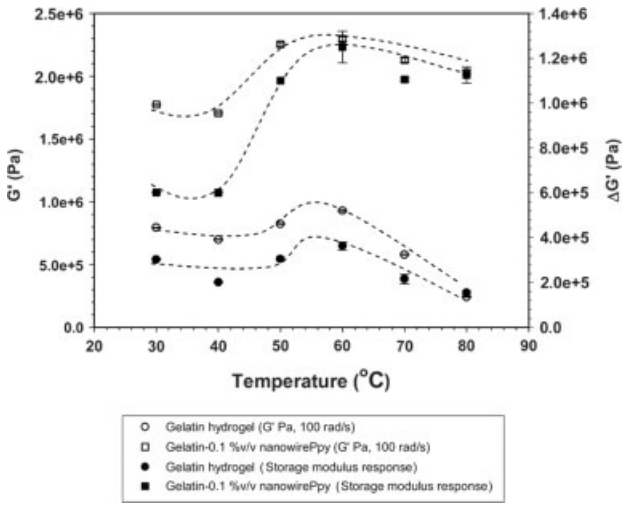

Figure 7. Effect of concentration of particles on the storage modulus (G') and the storage modulus response ($\Delta G'$) at various temperatures (sample diameter 30 mm, gel thickness 1.405 mm, 0.15% strain, electric field strength 800 V mm^{-1}, frequency 100 rad s^{-1}).

increment drastically increases with temperature consistent with classical network theory (40–60 °C). From the results shown, the electromechanical responses of nanowire-Ppy/gelatin hydrogel are mainly improved in terms of storage modulus response ($\Delta G'$) via Ppy polarization. With the presence of nanowire-Ppy, $G'_{800V/mm}$ and $\Delta G'$ at any temperature are higher than those of the pure gelatin hydrogel since the nanowire-Ppy acts as a filler and creates a wire-to-wire dipole interaction under an electric field.

Deflection of nanowire-Ppy/gelatin hydrogels

The deflection of the pure gelatin and nanowire-Ppy/gelatin hydrogels was studied by vertically suspending the films in a silicone oil bath; a DC electric field was applied horizontally between two parallel flat copper electrodes, as shown in Fig. 8. The amount of deflection at a specified electric field strength is defined by the geometrical parameters – d, l and θ – which are illustrated in Fig. 8. The tip displacement of the film was recorded by a digital video recorder (Sony, Handicam HR1). Figures 9(a)–9(c) show the bending of the pure gelatin and the nanowire-Ppy/gelatin hydrogels immersed in the silicone oil with an electric field strength of 600 V mm^{-1}. Upon applying an electric field, the free lower end of the film deflects towards the anode side by an amount, depending on the field strength, that results from the effect of the non-symmetric charges. The pure gelatin hydrogel indicates an attractive interaction between the anode and the polarized carbonyl group, in which the gelatin structure possesses negative charge. The deflection distances of the pure gelatin and the nanowire-Ppy/gelatin hydrogels under the electric field are shown in Figs 10(a) and 10(b). The pure gelatin hydrogel shows greater deflection values than the nanowire-Ppy/gelatin hydrogels. The hydrogels start to deflect at lower critical electric field strengths: 25 V mm^{-1}, 300 V mm^{-1} and 400 V mm^{-1} for the pure gelatin hydrogel, the nanowire-Ppy(0.1 vol%)/gelatin and the nanowire-Ppy(1 vol%)/gelatin hydrogel, respectively. Moreover, the nanowire-Ppy/gelatin hydrogels show a lesser deflection response under an applied electric field than the pure gelatin hydrogel due to its initial higher rigidity, or its higher G'_o value.

Figures 10(a) and 10(b) show the deflection distances and the dielectrophoresis forces of the pure gelatin and the

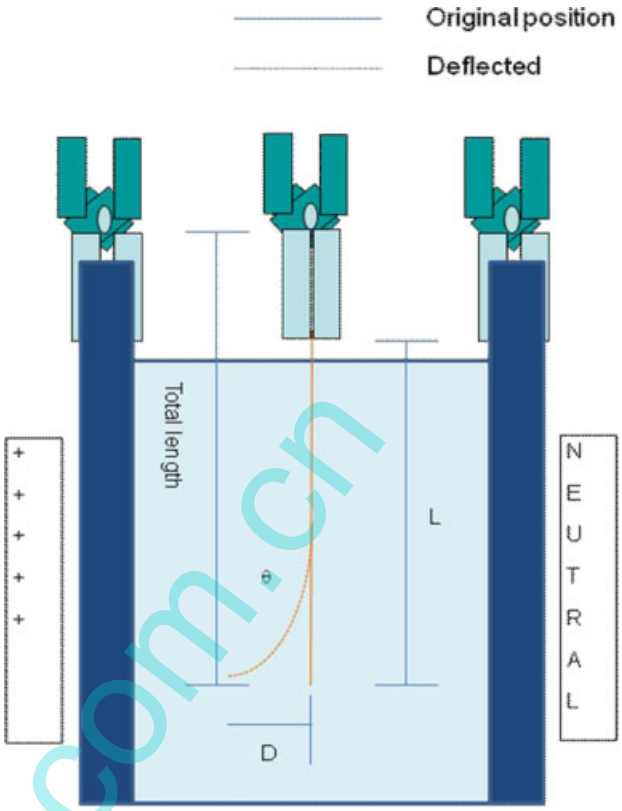

Figure 8. Schematic diagram of the apparatus used to observe the dielectrophoretics of the hydrogel samples.

nanowire-Ppy/gelatin hydrogels under an electric field. The deflection distances and dielectrophoresis forces of the pure gelatin and the nanowire-Ppy/gelatin hydrogels appear to increase stepwise with increasing electric field strength. The dielectrophoresis force at $E = 600$ V mm^{-1} for the pure gelatin hydrogel, the nanowire-Ppy(0.1 vol%)/gelatin hydrogel and the nanowire-Ppy(1.0 vol%)/gelatin hydrogel is 7.05, 6.60 and 1.60 mN, respectively. Surprisingly, the resultant dielectrophoresis forces of the nanowire-Ppy/gelatin hydrogels under the applied electric field are smaller than those of the pure gelatin hydrogel. It appears that the induced dipole moments generated by nanowire-Ppy counteract those of the pure gelatin. Under an applied electric field, pure gelatin hydrogel can polarize and generate non-symmetric negative charges. On the other hand, the nanowire-Ppy has strong positive charges attached on the main chains. Apparently, the presence of positive charge diminishes the non-symmetric negative charges generated within the gelatin matrix. Therefore, the bending and the dielectrophoresis forces of the nanowire-Ppy/gelatin hydrogels under an electric field are less.

In previous work, Thongsak *et al.*[33] reported the dielectrophoresis force of styrene–isoprene–styrene triblock copolymer (SIS D1114P): the maximum deflection distance and the dielectrophoresis force at $E = 600$ V mm^{-1} were 2.86 mm and 36.4 μN, respectively. Dai *et al.*[34] studied the bending force under an applied electric field of an ionic network membrane based on blends of water-soluble poly(vinyl alcohol) and highly ionic conductive poly(2-acrylamido-2-methyl-1-propane)sulfonic acid. The bending force of the blend was equal to 4.9 mN at $E = 40$ V mm^{-1}. Kunanuruksapong and Sirivat[35] studied the electromechanical response of an acrylic elastomer (AR70). The maximum deflection

Figure 9. Deflection of the hydrogels at $E = 0$ and 600 V mm^{-1}: (a) pure gelatin hydrogel; (b) 0.1 vol% nanowire-Ppy/gelatin hydrogel; (c) 1 vol% nanowire-Ppy/gelatin hydrogel. Note that the polarity of the electrode on the left-hand side is positive.

distance and dielectrophoresis force at an electrical strength of 225 V mm^{-1} was 12.41 mm and 0.367 mN, respectively. For the pure gelatin and nanowire-Ppy/gelatin hydrogels studied in this work, the maximum deflection distance and dielectrophoretic force were obtained for the pure gelatin hydrogel at $E = 600$ V mm^{-1}. They were 14.84 mm and 7.055 mN, respectively.

CONCLUSIONS

In this study, the electromechanical properties, the storage modulus response under oscillatory shear mode and the cantilever bending, of pure gelatin and nanowire-Ppy/gelatin hydrogels were investigated as functions of electric field strength and operating temperature. In the pure gelatin hydrogel and nanowire-Ppy/gelatin hydrogels with 0.01, 0.1, 0.5 and 1 vol%., the storage modulus (G'), the storage modulus response ($\Delta G'$) and the storage modulus sensitivity ($\Delta G'/G_o$) increase monotonically with increasing electric field strength up to 800 V mm^{-1}. The maximum storage modulus sensitivity was 104% for the nanowire-Ppy(0.1 vol%)/gelatin hydrogel at an electric field strength of 800 V mm^{-1}. The mechanism for the storage modulus response is the interaction between electrically polarized nanowire-Ppy which induces an electrostatic interaction and the effect of particles acting as fillers. In the presence of nanowire-Ppy, G' and $\Delta G'$ at any temperature investigated are higher than those of the pure gelatin hydrogel since the nanowire-Ppy acts as a filler and creates a wire-to-wire dipole interaction in an electric field. For the deflection measurement, the deflection distances and the dielectrophoresis forces of the pure gelatin and nanowire-Ppy/gelatin hydrogels increase monotonically with increasing electric field strength. In the case of the nanowire-Ppy(1 vol%)/gelatin hydrogel it possesses the lowest deflection response relative to the others due to its initially higher rigidity or its higher G'_o value. However, the nanowire-Ppy(0.1 vol%)/gelatin hydrogel is shown overall here to be more electroactive than the pure gelatin hydrogel.

ACKNOWLEDGEMENTS

The authors would like to acknowledge financial support from the Conductive and Electroactive Polymers Research Unit of Chulalongkorn University; the Thailand Research Fund (TRF-BRG); the Royal Thai Government; Nanotec; the National Center

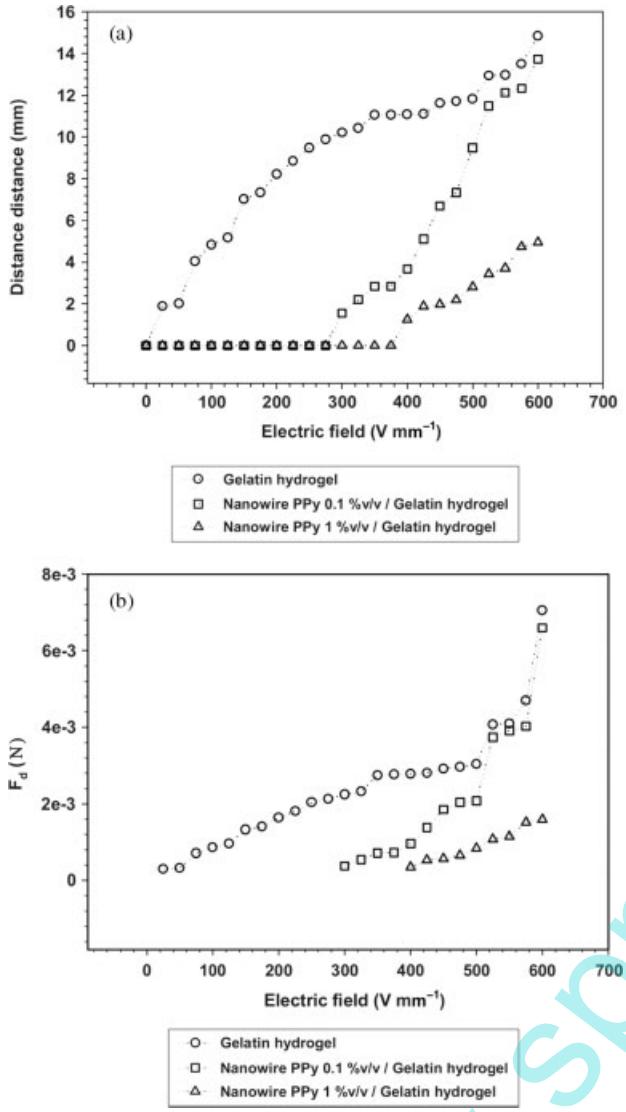

Figure 10. (a) Deflection distances of the gelatin hydrogel, the 0.1 vol% nanowire-Ppy/gelatin hydrogel, and the 1 vol% nanowire-Ppy/gelatin hydrogel at various electric field strengths. (b) Dielectrophoretic force calculated through linear deflection theory.

of Excellence for Petroleum, Petrochemicals, and Advanced Materials; and the Petroleum and Petrochemical College (PPC), Chulalongkorn University. T. Tungkavet acknowledges a Doctoral Scholarship received from the Thailand Graduate Institute of Science and Technology (TGIST) (TG-33-09-53-003D).

REFERENCES

1 Shahinpoor M, Bar-Cohen Y, Simpson JO and Smith J, *Smart Mater Struct* **7**:R15–R30 (1998).
2 Calvert P and Liu Z, *Acta Mater* **46**:2565–2571 (1998).
3 MacDiarmid AG, Chiang JC, Halpern M, Huang WS, Mu SL, Somasiri NL, *et al*, *Mol Cryst Liq Cryst* **121**:173–180 (1985).
4 Zhang QM, Bharti V and Zhao X, *Science* **280**:2101–2104 (1998).
5 Perline RE, Kornbluh RD and Joseph JP, *Sensor Actuat Phys A* **64**:77–85 (1998).
6 Kim J and Seo YB, *Smart Mater Struct* **11**:355–360 (2002).
7 Bar-Cohen Y, *Electroactive Polymer (EAP) Actuators as Artificial Muscles: Reality, Potential, and Challenges*, SPIE, Washington (2001).
8 Koyama K, Minagawa K, Watanabe T, Kumakura Y and Takimoto J, *J Non-Newtonian Fluid Mech* **58**:195–206 (1995).
9 Yang XJ, Zheng PJ, Cui ZD, Zhao NQ, Wang YF and Yao KD, *Polym Int* **44**:448–452 (1997).
10 Marois Y, Chakfe N, Deng X, Marois M, How T, King M, *et al*, *Biomaterials* **16**:1131–1139 (1995).
11 Ross-Murphy SB, *Polymer* **33**:2622–2627 (1992).
12 Haider S, Park SY, Saeed K and Farmer BL, *Sensor Actuat B: Chem* **124**:517–528 (2007).
13 Puvanatvattana T, Chotpattananont D, Hiamtup P, Niamlang S, Sirivat A and Jamieson AM, *React Funct Polym* **66**:1575–1588 (2006).
14 Skotheim TA, Elsenbaumer RL and Reynolds JR, *Handbook of Conducting Polymers*, Marcel Dekker, New York, p. 483 (1998).
15 Yang Y and Wan M, *J Mater Chem* **11**:2022–2027 (2001).
16 Athawale AA, Katre PP, Bhagwat SV and Dhamane AH, *J Appl Polym Sci* **108**:2872–2875 (2008).
17 Waghuley SA, Yenorkar SM, Yawale SS and Yawale SP, *Sensor Actuat B: Chem* **128**:366–373 (2008).
18 Duchet J, Legras R and Demousteir-Champagne S, *Synthetic Met* **98**:113–122 (1998).
19 He C, Yang C and Li Y, *Synthetic Met* **139**:539–545 (2003).
20 Sato T, Watanabe H and Osaki K, *Macromolecules* **29**:6231–6239 (1996).
21 Timoshenko SP and Goodier JN, *Theory of Elasticity*, McGraw-Hill, Auckland (1970).
22 Prissanaroon W, Ruangchuay L, Sirivat A and Schwank J, *Synthetic Met* **114**:65–72 (2000).
23 Diaz F and Hall B, *IBM J Res Dev* **27**:342–347 (1983).
24 Street GB, Lindsey SE, Nazzal AI and Wynne KJ, *Mol Cryst Liq Cryst* **118**:137–148 (1985).
25 Shen Y and Wan M, *Synthetic Met* **96**:127–132 (1998).
26 Kwon WJ, Suh DK, Chin BD and Yu JW, *J Appl Polym Sci* **110**:1324–1329 (2008).
27 Martin CR, *Science* **266**:1961–1966 (1994).
28 Shiga T, *Deformation and Viscoelastic Behavior of Polymer Gels in Electric Fields, Advances in Polymer Science*, Springer-Verlag, Berlin, p. 134 (1997).
29 Liu B and Shaw TM, *J Rheol* **45**:641–657 (2001).
30 Kunanuruksapong R and Sirivat A, *Mat Sci Eng A* **454–455**:453–460 (2007).
31 Bigi A, Panzavolta S and Rubini K, *Biomaterials* **25**:5675–5680 (2004).
32 Fraga AN and Williams RJJ, *Polymer* **26**:113–118 (1985).
33 Thongsak K, Kunanuruksapong R, Sirivat A and Lerdwijitjarud W, *Mat Sci Eng A* **527**:2504–2509 (2010).
34 Dai CA, Kao A, Chang C, Tsai W, Chen W, Liu W, *et al*, *Sensor Actuat A-Phy* **155**:152–162 (2009).
35 Kunanuruksapong R and Sirivat A, *Curr Appl Phys* **11**:393–401 (2011).